Physics Letters B 779 (2018) 324–330

Contents lists available at ScienceDirect

Physics Letters B

www.elsevier.com/locate/physletb

The nuclear magnetic moment of ^{208}Bi and its relevance for a test of bound-state strong-field QED

S. Schmidt [a,*,1], J. Billowes [b], M.L. Bissell [b], K. Blaum [c], R.F. Garcia Ruiz [b], H. Heylen [c], S. Malbrunot-Ettenauer [d], G. Neyens [e], W. Nörtershäuser [a], G. Plunien [f], S. Sailer [c,g], V.M. Shabaev [h], L.V. Skripnikov [h,i], I.I. Tupitsyn [h,j], A.V. Volotka [h,k], X.F. Yang [e]

[a] Institut für Kernphysik, Technische Universität Darmstadt, 64289 Darmstadt, Germany
[b] School of Physics and Astronomy, The University of Manchester, Manchester, M13 9PL, United Kingdom
[c] Max-Planck-Institut für Kernphysik, 69117 Heidelberg, Germany
[d] Experimental Physics Department, CERN, 1211 Geneva 23, Switzerland
[e] KU Leuven, Instituut voor Kern-en Stralingsfysica, 3001 Leuven, Belgium
[f] Institut für Theoretische Physik, TU Dresden, 01062 Dresden, Germany
[g] Technische Universität München, 80333 München, Germany
[h] Department of Physics, St. Petersburg State University, 199034 St. Petersburg, Russia
[i] National Research Centre "Kurchatov Institute", B.P. Konstantinov Petersburg Nuclear Physics Institute, Gatchina, Leningrad District 188300, Russia
[j] Center for Advanced Studies, Peter the Great St. Petersburg Polytechnic University, 195251 St. Petersburg, Russia
[k] Helmholtz-Institut Jena, 07743 Jena, Germany

ARTICLE INFO

Article history:
Received 12 November 2017
Received in revised form 9 February 2018
Accepted 12 February 2018
Available online 14 February 2018
Editor: D.F. Geesaman

Keywords:
Nuclear magnetic moment
Bismuth
Hyperfine anomaly
Specific difference
Quantum electrodynamics
Laser spectroscopy

ABSTRACT

The hyperfine structure splitting in the $6p^3\,{}^4S_{3/2} \rightarrow 6p^2 7s\,{}^4P_{1/2}$ transition at 307 nm in atomic ^{208}Bi was measured with collinear laser spectroscopy at ISOLDE, CERN. The hyperfine A and B factors of both states were determined with an order of magnitude improved accuracy. Based on these measurements, theoretical input for the hyperfine structure anomaly, and results from hyperfine measurements on hydrogen-like and lithium-like ^{209}Bi$^{80+,82+}$, the nuclear magnetic moment of ^{208}Bi has been determined to $\mu(^{208}\mathrm{Bi}) = +4.570(10)\,\mu_N$. Using this value, the transition energy of the ground-state hyperfine splitting in hydrogen-like and lithium-like ^{208}Bi$^{80+,82+}$ and their specific difference of $-67.491(5)(148)$ meV are predicted. This provides a means for an experimental confirmation of the cancellation of nuclear structure effects in the specific difference in order to exclude such contributions as the cause of the *hyperfine puzzle*, the recently reported 7-σ discrepancy between experiment and bound-state strong-field QED calculations of the specific difference in the hyperfine structure splitting of ^{209}Bi$^{80+,82+}$.

1. Introduction

Since its development in 1947, the theory of (bound-state) quantum electrodynamics (BS-QED), a major keystone within the standard model of physics, has an impressive and long history of success [1–4] and has so far mastered all tests in light systems [5,6] with unprecedented accuracy. In contrast, first attempts to probe BS-QED in the regime of the heaviest elements, in particular by using heavy highly charged ions (HCIs), are much less accurate [7–9]. The best tests performed so far reached accuracies at the level of a few permille, even though the sensing power of the bound electron to QED effects is strongly enhanced – HCIs are like a magnifier for QED related contributions. Besides the measurements of the Lamb-shift [10–12] and the Landé g-factor [13–16] in HCIs, one promising quantity to access this non-perturbative regime of BS-QED is the ground-state hyperfine structure (hfs) splitting in hydrogen-like (H-like) ions, nowadays accessible by high-precision laser spectroscopy.

Previous direct tests of BS-QED via the transition energy of various ground-state hfs splittings in H-like ions [17–19] could not be exploited due to the large uncertainty in the theoretical predictions, mainly arising from the magnetic moment distribution over the finite nuclear size, the Bohr-Weisskopf effect [20]. It was sug-

* Corresponding author.
E-mail address: stefanschmidt@uni-mainz.de (S. Schmidt).
[1] Present address: Institut für Physik & Exzellenzcluster PRISMA, Johannes Gutenberg-Universität Mainz, 55122 Mainz, Germany.

https://doi.org/10.1016/j.physletb.2018.02.024

gested that the combination of the hfs splittings $\Delta E^{(1s)}$ of H-like and $\Delta E^{(2s)}$ of Li-like systems in the so-called specific difference $\Delta' E = \Delta E^{(2s)} - \xi \Delta E^{(1s)}$ would yield a conclusive test of BS-QED in strong magnetic fields [21]. This is because if the parameter ξ is suitably chosen, nuclear effects will cancel in $\Delta' E$. A first measurement of the specific difference in ^{209}Bi was reported in [22], but did not provide sufficient experimental accuracy to become sensitive to the remaining QED contributions [22,23]. With recent experimental improvements [24], the specific difference was determined with more than an order of magnitude improved accuracy [25]. However, a large discrepancy between the specific difference extracted from the hfs splitting in H-like and Li-like ^{209}Bi and theoretical expectation was reported, establishing the *hyperfine puzzle* of BS-QED. This result challenges BS-QED, but might also be explained by a value for the nuclear moment of ^{209}Bi which deviates from literature, as it enters linearly into the theoretical value for the specific difference. As discussed in Ref. [24], there are three possible reasons for the *hyperfine puzzle*: (i) The magnetic moment of ^{209}Bi is different from the literature value, (ii) the elimination of nuclear structure contributions in the specific difference $\Delta' E$ does not work as expected or (iii) QED fails. Please note that it is not excluded that the discrepancy is caused by more than one of these reasons. Therefore, all points should be addressed in future experiments.

Explanation (i) has been checked by improved high precision calculations of the shielding and chemical shift corrections for available and new NMR data. Results have been published in [26] and do indeed agree with the storage ring results within uncertainties. However, the extraction of the nuclear moment depends again on advanced theoretical calculations of the shielding constant which is, from a fundamental point of view, not completely satisfying taking into account remaining uncertainties of molecular calculations. Therefore, a strong need remains to measure magnetic moments of such nuclei on a bare or hydrogen-like system, where shielding effects are absent or under very good control.

In order to check (ii) we suggest to measure the specific difference of ^{208}Bi and provide here the crucial information for this experiment. From a nuclear physics point of view, the nuclear magnetic moment distribution in ^{208}Bi must be considerably different from that of ^{209}Bi. The latter has a single proton in the $h_{9/2}$ shell outside of the ^{208}Pb core, while in the former there is an additional contribution from a $p_{1/2}$ neutron hole in the ^{208}Pb core. This, and their large magnetic moments make these isotopes an ideal pair to check the independence of $\Delta' E$ from the nuclear moment contribution. To predict the specific difference of ^{208}Bi, which is required for this test, the magnetic moment of this isotope must be determined with better accuracy. The most accurate values for the magnetic moments of short-lived isotopes are obtained from hyperfine structure measurements but require a well-known magnetic moment of a stable isotope. In addition, one has to include predictions for the hyperfine structure anomaly in a given atomic state. In order to disentangle (i) from (ii), we assume that the observed discrepancy in $\Delta' E$ is solely due to a wrong magnetic moment. In this case, we can use the measured specific difference and extract the magnetic moment of ^{209}Bi required to bring experiment into agreement with theory. Based on this assumption, we calculate the hyperfine structure splittings and the specific difference for H-like and Li-like ^{208}Bi with respect to the new value. If our predictions will be in accordance with the measurements, explanation (ii) can be ruled out within the accuracy of the results.

Here, we have measured the hfs splitting of the $^4S_{3/2}$ and $^4P_{1/2}$ states in atomic ^{208}Bi by means of collinear laser spectroscopy performed at the ISOLDE facility at the European Center for Nuclear Research (CERN). In the analysis we also include hyperfine structure anomaly calculations to extract the most precise value of the nuclear magnetic moment of the bismuth isotope ^{208}Bi. Based on the improved value, a reliable prediction of the ground-state hfs splitting in H-like and Li-like ^{208}Bi and their specific difference is made. If those values will be confirmed in upcoming laser-spectroscopy experiments on ^{208}Bi$^{80+,82+}$, the proposed cancelation of the nuclear magnetic moment distribution in the specific difference can be firmly established.

2. Experimental setup

The measurements on the long-lived bismuth isotope ^{208}Bi (half-life of 3.7×10^5 y) with respect to a reference isotope (^{209}Bi) were performed at the radioactive ion beam facility ISOLDE, located at CERN. A schematic of the on-line isotope separator and the collinear laser spectroscopy experiment (COLLAPS) [27–29] is shown in Fig. 1. In brief, the bismuth isotopes are produced in the target section by impinging high-energy proton pulses at 1.4 GeV on a uranium carbide target. The target material itself is heated to about 2200 °C to promote the diffusion process of the chemical compounds in the target material as well as the effusion through the transfer line towards the ionization region. Element selective ionization is performed on the neutral atoms using a (multi-step) resonance ionization scheme [30], followed by mass-selection with the High-Resolution Mass Separator (HRS).

Before the injection of the almost mono-isotopic ion beam into the collinear beamline apparatus, the ions are stopped inside a gas-filled radiofrequency quadrupole (RFQ) trap for ion bunching, cooling and accumulation. The voltage applied to the RFQ defines the starting potential of the ion bunch for collinear laser spectroscopy. It is set to about 30 kV in order to accomplish the mandatory velocity compression [27], which sets the basis for high-resolution experiments of this kind.

After releasing the bismuth ions from the RFQ, they enter the COLLAPS beamline, where they are collinearly superimposed with a continuous wave laser beam at 307 nm provided by a frequency-doubled Matisse dye-laser, stabilized to a high-finesse wavemeter (WS-10) [31]. The beamline consists of a 10° electrical bender, ion optical components to guide the beam (these components are not shown in Fig. 1), a sodium vapor charge-exchange cell (CEC) and an optical detection region (ODR), mounted perpendicular relative to the propagation direction of the ion beam. The post-acceleration voltage (positive or negative) applied to the CEC allows for fast and precise Doppler-tuning of the ion bunch. After neutralization in the CEC, the hfs of the bismuth atoms (see level scheme in Fig. 1 for details) can be probed. Light scattered by the atoms is focused by a two lens system on a photomultiplier tube. For background suppression, the photomultiplier tubes were gated for 15 µs with respect to the time-of-flight window of the ion bunches.

3. Experimental results

The hfs splitting of the two bismuth isotopes ^{209}Bi and ^{208}Bi were alternately measured within a six-hour measurement campaign. In total seven spectra were recorded, four in the case of ^{208}Bi and three for ^{209}Bi. Each spectrum was taken with an accumulation time between thirty and sixty minutes. The obtained hfs spectra (see Fig. 2 for ^{208}Bi) were fitted using a sixfold line-profile of individual amplitudes and with their positions correlated through the hfs which depends on the magnetic and quadrupole hyperfine parameters [32]. Best agreement was found using a Lorentzian- or a Voigt-profile with a dominating Lorentzian part. Thus, the former one was used in the following analysis. The residuals (not displayed) show no indication for *satellite peaks* [33].

During the measurement campaign, the starting potential, the ion optical settings as well as the laser frequency were kept con-

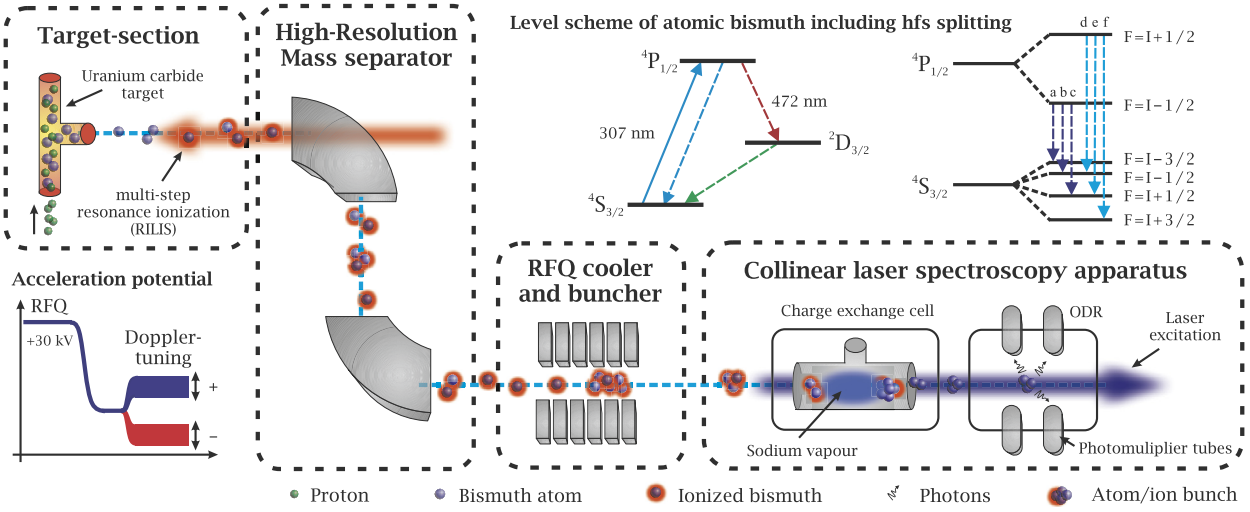

Fig. 1. Schematic overview of the collinear laser spectroscopy apparatus at ISOLDE, CERN including the target-section, the High-Resolution Mass separator, the RFQ and the COLLAPS beamline (see text for further details). The level scheme at the top right of this figure shows the laser transition as well as the different decay branches. The scheme in the lower left part sketches the two acceleration potentials applied to either the RFQ and to the charge exchange cell.

Table 1
Hfs coefficients of bismuth. The values for ^{208}Bi contain both statistical and systematic uncertainties, which were added in quadrature. Values are given in MHz. Bold printed values were used to calculate the hfs anomaly.

	I	$A_j[^4S_{3/2}]$ (MHz)	$B_j[^4S_{3/2}]$ (MHz)	$A_j[^4P_{1/2}]$ (MHz)	Reference
^{209}Bi	9/2	**−446.942(1)**	−304.654(2)	+4920.8(0.6) +4921.9(5.4)	[34,37,38]
		−446.89(31)	−305.2(5.7)	**+4922.3(2.0)**	[this work]
^{208}Bi	5	−453(5)	−416(45)	+4932(14)	[37]
		−446.05(32)	−358.6(3.9)	**+4925.6(1.8)**	[this work]

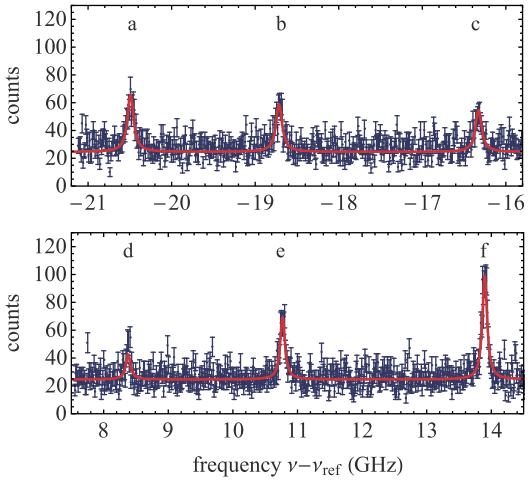

Fig. 2. Typical hfs spectra of ^{208}Bi relative to a reference frequency ν_{ref}. The individual hyperfine transitions are labeled as displayed in Fig. 1. The upper panel shows the hyperfine transitions a–c with decreasing peak intensities according to the matrix elements of the dipole operator (Wigner-6j symbol). The lower panel displays the transition triplet d–f.

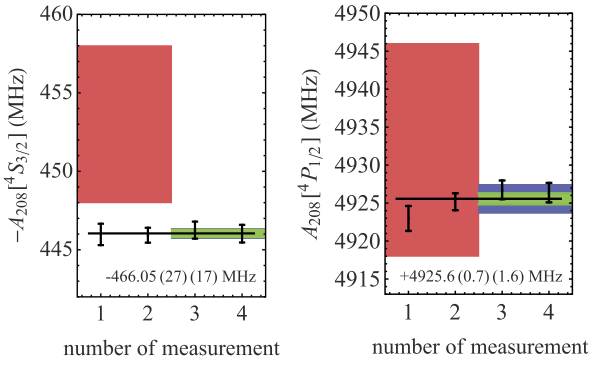

Fig. 3. Hyperfine coefficients of ^{208}Bi. The red shaded bands represent the literature values. The statistical and the combined statistical and systematic uncertainties are given in green and blue, respectively. The black lines correspond to the mean values. (For interpretation of the colors in the figure(s), the reader is referred to the web version of this article.)

stant. To cover a large frequency range, the acceleration voltage was alternately scanned around a negative and positive offset voltage provided by two individual Fluke power supplies of inverted polarity as sketched in Fig. 1.

From the fit the hyperfine $A_i[j]$ and $B_i[j]$ coefficients could be extracted for every spectrum. In this notation, the index j represents the given atomic state (fine structure level) of the individual isotope i. The consistency of the obtained results is illustrated in Fig. 3. Since the hyperfine coefficients $A_{209}[^4S_{3/2}]$ and $B_{209}[^4S_{3/2}]$ are known to high accuracy [34], these values have been used to deduce experimental parameters such as voltage divider ratios, following the procedure presented in [35]. The final results of the hyperfine coefficients including systematic uncertainties are presented in Table 1. They have been calculated according to the formalism presented in [27]. To be conservative, the statistical uncertainty represents the larger value of the calculated internal and external error [36] of the mean value, as presented in Fig. 3. Hereby, the internal error results from the error propagation of the individual uncertainties, whereas the external error is calculated from the sum of the residuals, weighted by their uncertainties. The $A_{208}[^4P_{1/2}]$ factor agrees with the previous literature value, but is about 8 times more precise, whereas the values for the $A_{208}[^4S_{3/2}]$ and $B_{208}[^4S_{3/2}]$ factors slightly deviate from literature, while being 15 and 12 times more precise, respectively.

4. Nuclear magnetic moment of ^{208}Bi

The current literature value for the nuclear magnetic moment of ^{208}Bi, $\mu(^{208}\mathrm{Bi}) = +4.578(13)\,\mu_N$ [37], was calculated using the hfs constant of the $6p^2 7s\,^4P_{1/2}$ state in atomic bismuth with respect to the reference isotope ^{209}Bi. This is based on the fact that for a point-like nucleus the ratio of the hyperfine parameter A and the nuclear g factor $\sim \mu_I/I$ should be constant for all isotopes in a chain. However, the spatial distribution of the magnetic moment and the charge inside a finite-size nucleus leads to small deviations from this relation, which is called the hfs anomaly $^1\Delta^2$ between the isotopes 1 and 2

$$\frac{A_1}{A_2} = \frac{\mu_1 I_2}{\mu_2 I_1}\left(1 + {}^1\Delta^2\right). \tag{1}$$

In principle Eq. (1) can be used for the determination of the nuclear magnetic moment of one isotope, provided that the nuclear magnetic moment of the other isotope and the hfs anomaly are known to the required accuracy. Unfortunately, this is usually not the case, since the evaluation of the hfs anomaly requires the application of an elaborate microscopic nuclear model. The uncertainty of such an evaluation is generally rather large. For ^{208}Bi and ^{209}Bi this anomaly is mainly caused by the nuclear magnetization distribution referred to as the Bohr-Weisskopf effect. Since the hfs anomaly was ignored in [37], the final uncertainty of the reported value remained unclear. With the accuracy for the hfs constant(s) obtained here, we cannot neglect the anomaly. Instead we combine theoretical calculations with our experimental results in order to obtain an accurate value of the magnetic moment with a reliable uncertainty. We also provide a new reference value for the nuclear magnetic moment of ^{209}Bi by using the outcome of the measurements of the specific difference $\Delta' E_{\mathrm{exp}}$ in the H-like and Li-like systems (see Eq. (5)). This new value also enters linearly into the calculations of the nuclear magnetic moment of ^{208}Bi.

It is important to note that for heavy atoms the densities of all s and $p_{1/2}$ one-electron orbitals, which mainly contribute to the hfs anomaly, are proportional to each other in the nuclear region [21,39]. Thus, the ratio of the hyperfine structure anomalies $^1r^2[a,b] \equiv \frac{^1\Delta^2[a]}{^1\Delta^2[b]}$ in two states ($j = a, b$) for an isotope pair ($i = 1, 2$) should be approximately identical for different nuclear models and, therefore, can be calculated to good accuracy. In addition, a set of $A_i[j]$ factors measured in two atomic states and for two isotopes are combined to obtain the so-called differential hyperfine structure anomaly $^1\delta^2[a,b]$ according to

$$\frac{A_1[a]}{A_2[a]}\frac{A_2[b]}{A_1[b]} = \frac{\left(1 + {}^1\Delta^2[a]\right)}{\left(1 + {}^1\Delta^2[b]\right)} = 1 + {}^1\delta^2[a,b]. \tag{2}$$

By using these definitions we obtain the hfs anomaly in an electronic state b based on the experimental value for the differential hfs anomaly and the calculated ratio $^1r^2[a,b]$, according to

$$\Delta[b] = \frac{\delta[a,b]}{r[a,b] - \delta[a,b] - 1}. \tag{3}$$

Here, we have dropped the superscripts referring to the isotopes in $^{209}\Delta^{208} = \Delta$ (similar for δ and r) since in the following we will exclusively consider the isotope pair ^{208,209}Bi. In Section 5, Eq. (2) and (3) will be also used to obtain relations between the hyperfine structure anomalies in the two states of atomic bismuth that have been determined in our experiment and the $1s$ and $2s$ states in H-like and Li-like Bi, respectively, in order to obtain the most precise values for the hyperfine splittings in the highly charged bismuth ions.

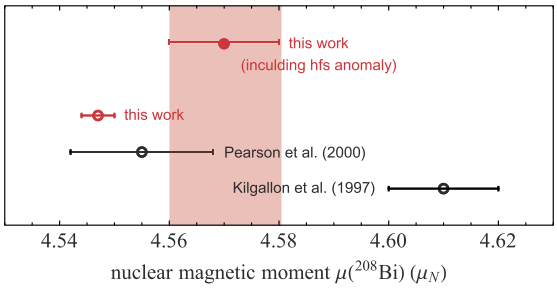

Fig. 4. Evolution of experimental values of the nuclear magnetic moment of ^{208}Bi. The values for the nuclear magnetic moment excluding the hfs anomaly, but corrected for the new magnetic moment $\mu(^{209}\mathrm{Bi}) = +4.0900(15)\,\mu_N$ as extracted from [25] according to Eq. (5), are shown in open symbols.

Our calculations employing the configuration-interaction Dirac–Fock–Sturm method [40] and the relativistic multireference coupled cluster method [41–43] yield

$$r[^4S_{3/2}, {}^4P_{1/2}] = 1.54(14). \tag{4}$$

By inserting this value into Eq. (3) we obtain the hfs anomaly of the $^4P_{1/2}$ state $\Delta[^4P_{1/2}] = 0.0049(21)$, where in addition we have used our values for $A_i[j]$ and the more precise value $A_{209}[^4S_{3/2}]$ for the ground state of ^{209}Bi taken from [34] (printed in bold in Table 1).

As the final step in order to obtain an accurate value for the nuclear magnetic moment of ^{208}Bi, the nuclear magnetic moment of ^{209}Bi is required. As discussed in the introduction, we consider the literature value obtained from NMR in $Bi(NO_3)_3$ solutions (see [44–47]) as unreliable since the molecular environment contribution to the chemical shift and its uncertainty was strongly underestimated [26]. Therefore, we prefer to use a new value extracted from the experimentally obtained specific difference $\Delta' E_{\mathrm{exp}}$ [25], the theoretical prediction $\Delta' E_{\mathrm{theo}}$ [48] and the value of $\mu(^{209}\mathrm{Bi})_{\mathrm{NMR}}$ from [46] which has been used to calculate $\Delta' E_{\mathrm{theo}}$. Since the specific difference is proportional to the nuclear magnetic moment, a value of

$$\mu(^{209}\mathrm{Bi}) = \frac{\Delta' E_{\mathrm{exp}}}{\Delta' E_{\mathrm{theo}}}\mu(^{209}\mathrm{Bi})_{\mathrm{NMR}} \tag{5}$$

brings the theoretical prediction into agreement with experiment. The result of $\mu(^{209}\mathrm{Bi}) = +4.0900(15)\,\mu_N$ will now be used to determine the nuclear magnetic moment of ^{208}Bi and to predict the hyperfine splittings in Li-like and H-like systems.[2] Please note that these predictions are therefore not affected anymore by a possible wrong magnetic moment of ^{209}Bi in literature and can thus be used as a sensitive test for the elimination of the Bohr-Weisskopf effect in $\Delta' E$, which has not been proven experimentally so far.

Following the procedure of [37] and neglecting the hfs anomaly in Eq. (1), we would obtain $\mu(^{208}\mathrm{Bi}) = +4.547(3)\,\mu_N$, as depicted in Fig. 4 (red open symbol). This value is about 5 times more precise than the previous literature value, which yields $\mu(^{208}\mathrm{Bi}) = +4.555(13)\,\mu_N$ using the new reference value $\mu(^{209}\mathrm{Bi})$. However, by taking into account the calculated value for $\Delta[^4P_{1/2}]$ and using Eq. (1), the nuclear magnetic moment of ^{208}Bi was found to be

$$\mu(^{208}\mathrm{Bi}) = +4.570(10)\,\mu_N, \tag{6}$$

[2] The value is also in good agreement with the new determination of the magnetic moment from NMR that has been published in parallel in [26].

which is clearly limited in accuracy due to the hfs anomaly and the experimental uncertainty of $A_{208}[^4S_{3/2}]$. This value nevertheless represents the most precise value for the nuclear magnetic moment of ^{208}Bi and deviates by about two times the combined uncertainty from the nuclear magnetic moment obtained neglecting the hfs anomaly. Based on this value we can now predict the ground-state hfs splitting and the specific difference of ^{208}Bi$^{80+,\,82+}$.

5. Ground state hyperfine splitting in ^{208}Bi^{80+} and ^{208}Bi^{82+}

Due to the high magnetic field of the nucleus experienced by the valence electron in H-like and Li-like bismuth, the ground state ($^2S_{1/2}$) hyperfine structure displays a large energy splitting, which is accessible by standard laser systems. Based on the results of the hfs coefficients for the $^4S_{3/2}$ and $^4P_{1/2}$ states and the new value for the nuclear magnetic moment of ^{208}Bi presented in this work, the ground state hyperfine splittings $\Delta E^{(1s)}$ (H-like) and $\Delta E^{(2s)}$ (Li-like) have been evaluated using two different ways. In the first method, which we refer to as *semiempirical*, the hfs constants for H-like and Li-like Bi ions can be expressed in a similar way as the hfs coefficients of neutral bismuth, cf. Eq. (2), where we have used the $^4S_{3/2}$ or $^4P_{1/2}$ state of atomic bismuth and the states $1s$ or $2s$ of H- or Li-like bismuth, respectively. We have calculated the ratios of hfs anomalies and found out that they are very stable with respect to a change of the nuclear model. Our calculations yield

$$r[^4P_{1/2}, 1s] = 1.113(14),$$
$$r[^4P_{1/2}, 2s] = 1.035(13). \quad (7)$$

Knowing these ratios and the values of $A_{208}[^4P_{1/2}]$, $A_{209}[^4P_{1/2}]$, $\Delta[^4P_{1/2}]$ together with $A_{209}[1s]$ and $A_{209}[2s]$ from [25] we arrive to the following result for the hfs constants $A_{208}[1s] = 1018.2(7)$ meV and $A_{208}[2s] = 159.66(9)$ meV, which directly yields $\Delta E^{(1s)}$ and $\Delta E^{(2s)}$ (see Table 2).

Another way – *theoretical* – is based on rigorous calculations within the formalism presented in [21,48,49], where the individual contributions arising from the nuclear size, the magnetization distribution, and the QED ($x_{\rm rad}$) corrections have been evaluated directly. For the calculation of the magnetization distribution correction, the Bohr-Weisskopf effect, we employ the nuclear shell model where the nuclear magnetic moment is possessed by an unpaired proton in the $1h_{9/2}$ state and an unpaired neutron in the $3p_{1/2}$ state [50]. Within this model the observed nuclear magnetic moment is reproduced by an adjustment of the spin g-factors of the unpaired nucleons. Here, we have used the nuclear magnetic moment of ^{208}Bi ($\mu(^{208}\text{Bi}) = +4.570(10)\,\mu_N$) together with the magnetic moment of one of the neighboring nuclei ($\mu(^{207}\text{Pb}) = +0.592583(9)\,\mu_N$, $\mu(^{207}\text{Bi}) = +4.0915(9)\,\mu_N$, $\mu(^{209}\text{Bi}) = +4.0900(15)\,\mu_N$, and $\mu(^{209}\text{Po}) = +0.68(8)\,\mu_N$) in order to adjust the spin g-factor of both nucleons. Averaging over four pairs of nuclei, the effective spin g-factors and their standard deviations are obtained to amount to 3.04(21) and −3.35(51) for the unpaired proton and neutron, respectively. The radial wavefunctions of the unpaired nucleons have been found as solutions of the Schrödinger equation with the Woods-Saxon potential. Following Ref. [51] the uncertainty of the Bohr–Weisskopf effect due to the employed model is estimated as 30% of its value.

In order to test the nuclear model utilized in the present study we compare the hfs anomalies $\Delta[1s]$ and $\Delta[2s]$ obtained theoretically and extracted semiempirically from the experiments on neutral bismuth. Knowing the ratios (7) and the hfs anomaly $\Delta[^4P_{1/2}]$ deduced in the preceding section, we immediately obtain the hfs anomalies for the $1s$ and $2s$ states to be 0.0044(19) and 0.0047(20), respectively. These values have to be compared with the predictions of the single particle nuclear model which are 0.0035 and 0.0038 for H- and Li-like cases, respectively. This comparison demonstrates a good agreement, what emphasizes the conformity of the model. The results for the hyperfine splittings in H-like and Li-like ^{208}Bi obtained using both ways, semiempirical and theoretical, are presented in Table 2. The theoretical values are obtained by summing the individual contributions which are also included in the table.

Table 2
The theoretical and semiempirical values of the ground-state hyperfine splitting in H-like and Li-like ^{208}Bi, including the individual theoretical contributions. In the total theoretical results the first uncertainty is mainly due to the Bohr-Weisskopf effect, while the second one is due to the uncertainty of the nuclear magnetic moment of $\mu(^{208}\text{Bi}) = +4.570(10)\,\mu_N$. All uncertainties were added in quadrature.

	$\Delta E^{(1s)}$ (meV)	$\Delta E^{(2s)}$ (meV)
Relativistic value	6427	1055.0
Nuclear size	−712(4)	−125.0(6)
Bohr-Weisskopf	−88(30)	−14.8(5.0)
One-electron QED	−33	−5.6
Interel.-int.		−32.7
Screened QED		0.2
Theoretical	5594(30)(12)	877.1(5.0)(1.9)
Semiempirical	5600(4)	878.1(5)

Table 3
Calculated contributions to the specific difference for ^{208}Bi. The first uncertainty is due to the uncalculated terms and remaining nuclear effects, while the second one is due to the uncertainty of the nuclear magnetic moment. All theoretical uncertainties were added in quadrature.

	$\Delta' E$ (meV)
Dirac value	−35.008
Interel.-int.	
$\sim 1/Z$	−33.017
$\sim 1/Z^2$	0.285
$\sim 1/Z^3$	−0.003(3)
One-electron QED	0.040
Screened QED	0.213(2)
Total	−67.491(5)(148)

In addition, we consider the specific difference $\Delta' E$ of the ground state hyperfine splitting of H-like and Li-like ions,

$$\Delta' E = \Delta E^{(2s)} - \xi \Delta E^{(1s)}, \quad (8)$$

where the parameter $\xi = 0.16886$ is chosen to cancel the Bohr-Weisskopf correction. The specific difference $\Delta' E$ has been directly calculated for ^{208}Bi, revealing a value of −67.491(5)(148) meV. Here, the second uncertainty is due to the uncertainty of the nuclear magnetic moment. The dependency of both uncertainties is purely linear, as $\Delta' E \sim \mu(^{208}\text{Bi})$. This illustrates the importance of an accurate knowledge of the nuclear magnetic moment for a future BS-QED test in ^{208}Bi, as now provided by this work. The individual contributions to the first (theoretical) uncertainty of the specific difference are presented in Table 3 and were added in quadrature. Here, we note that the nuclear effects and their uncertainties almost cancel and are therefore not listed in the table.

Experimentally, the new and more precise values for the transition wavelengths and $\Delta' E$ will (a) support the search for the hyperfine transitions in H-like and Li-like ions at the ESR in an upcoming experiment, (b) serve as an independent test that nuclear structure contributions are eliminated in $\Delta' E$ and (c) if successfully confirmed in an experiment it will demonstrate that the mag-

netic moment is indeed (most likely) the cause for the *hyperfine puzzle*. Additionally, this would establish a technique to accurately determine nuclear magnetic moments from the measurement of the hfs in H-like and Li-like heavy systems and $\Delta' E_{\text{theo}}$, which are independent from hfs anomalies and shielding corrections. In addition, the individual hfs splittings can be used to extract information about the magnetization distribution and to test nuclear models [52]. For instance, knowing the specific difference and individual 1*s* and 2*s* hfs splittings for ^{209}Bi [25] and assuming that the QED corrections are correct one may deduce not only the magnetic moment of ^{209}Bi but also the Bohr-Weisskopf correction, which, e.g., for the 1*s* state gives $\epsilon^{209}[1s] = 0.0098(7)$, where ϵ is defined similar as in [49]. Further, employing the value for the hfs anomaly $\Delta[1s]$ we obtain the Bohr-Weisskopf correction also for ^{208}Bi $\epsilon^{208}[1s] = 0.0142(20)$.

6. Conclusion

In this work, we have investigated the magnetic structure of ^{208}Bi by means of high-precision collinear laser spectroscopy. Using the stable bismuth isotope ^{209}Bi as an atomic reference to minimize systematic effects, the hyperfine-structure constants were measured to high accuracy, being more than one order of magnitude more precise than previous values in literature. The corresponding analysis of the nuclear magnetic structure revealed a nuclear magnetic moment of $\mu(^{208}\text{Bi}) = +4.570(10)\,\mu_N$, including hfs anomaly corrections for the first time. Moreover, we have obtained two predictions, semiempirical and theoretical, for the ground-state hyperfine transition energy in ^{208}Bi^{82+}, 5600(4) meV and 5594(30)(12) meV, and in ^{208}Bi^{80+}, 878.1(5) meV and 877.1(5.0)(1.9) meV, respectively, as well as for a specific difference, $\Delta' E = -67.491(5)(148)$ meV.

Based on these values, a new experiment is proposed to be carried out at the GSI Helmholtz Center for Heavy Ion Research. Production and storage of ^{208}Bi$^{80+,\,82+}$ in the experimental storage ring will allow a measurement of the specific difference of a radioactive isotope for the first time. Technical developments to increase the detection efficiency for this species are under way [53]. The results will give new insights in the fundamental nature of the electromagnetic interaction and will contribute to the solution of the *hyperfine puzzle*. Extending the measurements of the specific difference to the isotopic sequence in bismuth might also serve as a benchmark for nuclear structure calculations, especially towards an improved understanding of the Bohr-Weisskopf effect in the heaviest elements for the determination of nuclear magnetic moments.

Acknowledgements

The support and assistance from the ISOLDE technical group are gratefully acknowledged. This work was supported by the IAP-project P7/12, the FWO-Vlaanderen, GOA grant 15/010 from KU Leuven, the BMBF Contracts No. 05P15RDCIA and 05P15RDFAA, the Max Planck Society, the Science and Technology Facilities Council Consolidated Grant No. ST/L005794/1, the EU FP7 via ENSAR2 No. 654002, the RFBR (Grants No. 16-02-00334 and No. 16-32-60013 mol-a-dk), by the President of Russian Federation Grant (No. MK-2230.2018.2), by SPSU (Grants No. 11.40.538.2017, No. 11.42.666.2017 and No. 11.42.668.2017), and by SPSU-DFG (Grants No. 11.65.41.2017 and No. STO 346/5-1).

References

[1] W.E. Lamb, R.C. Retherford, Phys. Rev. 72 (3) (1947) 241.
[2] H.B.G. Casimir, Proc. K. Ned. Akad. Wet. 51 (7) (1948).
[3] G. Gabrielse, D. Hanneke, T. Kinoshita, M. Nio, B. Odom, Phys. Rev. Lett. 97 (3) (2006) 030802.
[4] D. Hanneke, S. Fogwell, G. Gabrielse, Phys. Rev. A 83 (5) (2011) 052122.
[5] S.G. Karshenboim, Phys. Rep. 422 (1) (2005) 1–63.
[6] W. Quint, Manuel Vogel (Eds.), Fundamental Physics in Particle Traps, vol. 256, Springer, 2014.
[7] D.A. Glazov, Y.S. Kozhedub, A.V. Maiorova, V.M. Shabaev, I.I. Tupitsyn, et al., Hyperfine Interact. 199 (2011) 71.
[8] A.V. Volotka, D.A. Glazov, G. Plunien, V.M. Shabaev, Ann. Phys. (Berlin) 525 (2013) 636.
[9] H.F. Beyer, V.P. Shevelko, Introduction to the Physics of Highly Charged Ions, CRC Press, 2016.
[10] T. Stöhlker, P.H. Mokler, F. Bosch, R.W. Dunford, F. Franzke, et al., Phys. Rev. Lett. 85 (15) (2000) 3109.
[11] A. Gumberidze, T. Stöhlker, D. Banasm, K. Beckert, P. Beller, et al., Phys. Rev. Lett. 94 (22) (2005) 223001.
[12] P. Beiersdorfer, H. Chen, D.B. Thorn, E. Träbert, Phys. Rev. Lett. 95 (23) (2005) 233003.
[13] J. Verdú, S. Djekić, S. Stahl, T. Valenzuela, M. Vogel, et al., Phys. Rev. Lett. 92 (9) (2004) 093002.
[14] S. Sturm, A. Wagner, B. Schabinger, J. Zatorski, Z. Harman, et al., Phys. Rev. Lett. 107 (2) (2011) 023002.
[15] A. Wagner, S. Sturm, F. Köhler, D.A. Glazov, A.V. Volotka, et al., Phys. Rev. Lett. 110 (3) (2013) 033003.
[16] F. Köhler, K. Blaum, M. Block, S. Chenmarev, S. Eliseev, et al., Nat. Commun. 7 (2016).
[17] I. Klaft, S. Borneis, T. Engel, B. Fricke, R. Grieser, et al., Phys. Rev. Lett. 73 (18) (1994) 2425.
[18] J.R. Crespo López-Urrutia, P. Beiersdorfer, D.W. Savin, K. Widmann, Phys. Rev. Lett. 77 (5) (1996) 826.
[19] P. Seelig, S. Borneis, A. Dax, T. Engel, S. Faber, et al., Phys. Rev. Lett. 77 (22) (1998) 4824.
[20] A. Bohr, V.F. Weisskopf, Phys. Rev. 77 (94) (1950).
[21] V.M. Shabaev, A.N. Artemyev, V.A. Yerokhin, O.M. Zherebtsov, G. Soff, Phys. Rev. Lett. 86 (2001) 3959.
[22] M. Lochmann, R. Jöhren, C. Geppert, Z. Andelkovic, D. Anielski, et al., Phys. Rev. A 90 (3) (2014) 030501.
[23] R. Sánchez, M. Lochmann, R. Jöhren, Z. Andelkovic, D. Anielski, et al., J. Phys. B 50 (8) (2017) 085004.
[24] J. Ullmann, Z. Andelkovic, A. Dax, W. Geithner, C. Geppert, et al., J. Phys. B 48 (2016) 144022.
[25] J. Ullmann, Z. Andelkovic, C. Brandau, A. Dax, W. Geithner, et al., Nat. Commun. 8 (2017) 15484.
[26] L.V. Skripnikov, S. Schmidt, J. Ullmann, C. Geppert, F. Kraus, et al., Phys. Rev. Lett. (2018), in print.
[27] A.C. Mueller, F. Buchinger, W. Klempt, E.W. Otten, R. Neugart, et al., Nucl. Phys. A 403 (2) (1983) 234–262.
[28] R. Neugart, Hyperfine Interact. 24 (1) (1985) 159–180.
[29] R. Neugart, J. Billowes, M.L. Bissell, K. Blaum, B. Cheal, et al., J. Phys. G 44 (6) (2017) 064002.
[30] B.A. Marsh, Rev. Sci. Instrum. 85 (2) (2014) 02B923.
[31] In this report, commercial products are only highlighted for technical clarity. It does not imply endorsement for a specific company by the authors, nor should it be seen as any kind of advertisement
[32] P. Campbell, I.D. Moore, M.R. Pearson, Prog. Part. Nucl. Phys. 86 (2016) 127–180.
[33] N. Bendali, H.T. Duong, P. Juncar, J.M. Saint Jalm, J.L. Vialle, J. Phys. B, At. Mol. Opt. Phys. 19 (2) (1986) 233.
[34] R.J. Hull, G.O. Brink, Phys. Rev. A 2 (3) (1970) 685.
[35] Ch. Gorges, K. Blaum, N. Frömmgen, Ch. Geppert, M. Hammen, et al., J. Phys. B, At. Mol. Opt. Phys. 48 (24) (2015) 245008.
[36] R.T. Birge, Phys. Rev. 40 (2) (1932) 207.
[37] M.R. Pearson, P. Campbell, K. Leerungnavarat, J. Billowes, I.S. Grant, et al., J. Phys. G, Nucl. Part. Phys. 108 (12) (2000) 1829.
[38] J. Kilgallon, M.R. Pearson, J. Billowes, P. Campbell, U. Georg, et al., Phys. Lett. B 405 (1) (1997) 31–36.
[39] V.M. Shabaev, D.A. Glazov, N.S. Oreshkina, A.V. Volotka, G. Plunien, et al., Phys. Rev. Lett. 96 (2006) 253002.
[40] I.I. Tupitsyn, A.V. Volotka, D.A. Glazov, V.M. Shabaev, G. Plunien, et al., Phys. Rev. A 72 (2005) 062503.
[41] M. Kállay, P.G. Szalay, P.R. Surján, J. Chem. Phys. 117 (2002) 980.
[42] M. Kállay, H.S. Nataraj, B.K. Sahoo, B.P. Das, L. Visscher, Phys. Rev. A 83 (2011) 030503.
[43] L.V. Skripnikov, J. Chem. Phys. 145 (2016) 214301.
[44] W.G. Proctor, F.C. Yu, Phys. Rev. 81 (1) (1951) 20.
[45] Y. Ting, D. Williams, Phys. Rev. 89 (3) (1953) 595.
[46] P. Raghavan, At. Data Nucl. Data Tables 42 (3) (1989) 189–291.
[47] T. Baştug, B. Fricke, M. Finkbeiner, W.R. Johnson, Z. Phys., D At. Mol. Clust. 37 (4) (1996) 281–282.

[48] A.V. Volotka, D.A. Glazov, O.V. Andreev, V.M. Shabaev, I.I. Tupitsyn, et al., Phys. Rev. Lett. 108 (7) (2012) 073001.
[49] V.M. Shabaev, in: H.F. Beyer, V.P. Shevelko (Eds.), Atomic Physics with Heavy Ions, Springer, 1999, pp. 139–159.
[50] H. Kopfermann, Kernmomente, Akademische Verlagsgesellschaft GmbH, Frankfurt, 1956.
[51] V.M. Shabaev, M. Tomaselli, T. Kühl, A.N. Artemyev, V.A. Yerokhin, Phys. Rev. A 56 (1) (1997) 252.
[52] R.A. Senkov, V.F. Dmitriev, Nucl. Phys. A 706 (2002) 351.
[53] M. Lestinsky, V. Andrianov, B. Aurand, V. Bagnoud, D. Bernhardt, et al., Eur. Phys. J. Spec. Top. 225 (5) (2016) 797–882.